Video imaging of walking myosin V by high-speed atomic force microscopy

doi: 10.1038/nature09450

Video imaging of walking myosin V by high-speed atomic force microscopy

Noriyuki Kodera[1,2], Daisuke Yamamoto[1,2], Ryoki Ishikawa[3], Toshio Ando[1,2]*
[1]Department of Physics, Kanazawa University, Kakuma-machi, Kanazawa 920-1192, Japan. [2]CREST, JST, Sanban-cho, Chiyoda-ku, Tokyo 102-0075, Japan. [3]Department of Molecular and Cellular Pharmacology, Gunma University Graduate School of Medicine, 3-39-22 Showa-machi, Maebashi 371-8511, Japan.
*To whom correspondence should be addressed. E-mail: tando@kenroku.kanazawa-u.ac.jp

The dynamic behaviour of myosin V molecules translocating along actin filaments has been mainly studied by optical microscopy. The processive hand-over-hand movement coupled with ATP hydrolysis was thereby demonstrated. However, the protein molecules themselves are invisible in the observations and have therefore been visualised by electron microscopy in the stationary states. Namely, the concomitant assessment of structure and dynamics has been unfeasible, a situation prevailing throughout biological research. Here, using high-speed atomic force microscopy, we directly visualise myosin V molecules walking along actin tracks. The high-resolution movies not only provide corroborative 'visual evidence' for previously speculated or demonstrated molecular behaviours including lever-arm swing but also reveal more detailed behaviours of the molecules, leading to a comprehensive understanding of the motor mechanism. Thus, the direct and dynamic high-resolution visualisation is a powerful new approach to studying the structure and dynamics of biomolecules in action.

Proteins are dynamic in nature and work at the single molecule level. Reflecting this fact, single-molecule fluorescence microscopy has widely been exploited to understand how proteins operate (see review[1]). However, what we can observe thereby is the dynamic behaviour of individual fluorescent spots (each being emitted from a fluorophore attached to a selected locus of the molecule), not of the protein molecules themselves. The structure of proteins has been studied by electron microscopy, x-ray crystallography, or NMR but the obtained structures are substantially static. To overcome this long-standing dilemma and enable to simultaneously record the structure and dynamics of functioning biomolecules, high-speed atomic force microscopy (HS-AFM) has been developed[2-5]. The recent significant improvement in its

performance has been demonstrated in a few imaging studies of proteins[6-8].

Myosin V (M5) is a two-headed processive motor and functions as a cargo transporter in cells (see review[9]). Facilitated by the processivity of the molecule[10,11], numerous single-molecule studies have demonstrated that it moves hand over hand with a ~36 nm advance[12,13] for every ATP hydrolysis[14]. However, the comprehensive depiction of the molecule in action has not yet been attained. Here, we applied HS-AFM to this highly dynamic protein to capture its minute dynamic behaviours. In addition to known and speculated behaviours, previously unappreciated ones clearly appeared in the molecular movies; (1) stomping-like brief detachment and rebinding of either head, (2) occasional unwinding of the coiled-coil tail of the two-head bound molecule followed by the leading lever-arm swing, indicating the presence of intramolecular tension responsible for the powerstroke, and (3) repeated conformational switching of the leading head by ADP binding and release. These findings lead to a better understanding of how M5 operates for its motor function.

Unidirectional processive movement

Partially biotinylated actin filaments were immobilised via streptavidin with a low surface density on biotin-containing lipid bilayers formed on a mica surface (Supplementary Fig. 1). To facilitate the weak sideways adsorption of M5-HMM (tail-truncated M5) onto the bilayer surface, a positively charged lipid (DPTAP, 5%) was included in the bilayer unless otherwise stated. This condition was necessary to clearly visualise M5-HMM molecules.

Fig. 1a shows images of M5-HMM moving processively with discrete ~36 nm steps (Supplementary Movie 1). A processive run almost always continued to the full extent of each imaging range used (*i.e.*, 4-16 steps). Typical long runs tracked by shifting the scan area are shown in Supplementary Movies 1c, d. In the two-head bound M5-HMM (head = motor domain + neck domain), the neck-motor domain junction appears smooth in the leading head (L-head) but is V-shaped in the trailing head (T-head) without exception (Fig. 1b), reflecting that the neck regions emerge from different parts of the motor domain. The short coiled-coil tail was mostly tilted toward the minus end of actin (arrows, Fig. 1a). These features are consistent with electron microscopy observations[15-17] and can be used to determine the actin polarity when bound M5-HMM is stationary.

Average translocation velocity (V) as a function of [ATP] was well fitted to $V = d_s/(1/k_1[\mathrm{ATP}] + 1/k_2)$, where d_s is the step size, k_1 is the second-order ATP binding rate constant, and k_2 is the first-order ADP dissociation rate constant (Supplementary Fig. 2).

The maximum velocity observed without DPTAP was similar to that measured by fluorescence microscopy[13,18], indicating the negligible effects of the tip-sample and surface-sample interactions on motor activity. When 5% DPTAP was included in the substrate surface, the values k_1 = 0.9 ± 0.3 μM^{-1} s^{-1} and k_2 = 7.2 ± 1.5 s^{-1} were obtained (Supplementary Table 1). The former agrees with previous reports, but the latter is about 70% of previously reported values (~11 s^{-1})[13,18], suggesting that the surface-sample interaction slightly reduces the rate of ADP release from the T-head.

Hand-over-hand movement

As observed above, the ~36 nm advance was completed within one frame (146.7 ms); therefore, the molecular process occurring during a step could not be resolved. However, additional streptavidin molecules placed on the substrate surface as moderate obstacles to the advance enabled visualising this process (Figs. 1c-e). After T-head detachment, the nearly straight leading neck swings from the reverse arrowhead (R-ARH) orientation to the arrowhead (ARH) orientation (clearly seen in Supplementary Movie 2), confirming the swinging lever-arm motion initially proposed for muscle myosin[19]. The detached T-head rotationally diffused around the advancing neck-neck junction (no translational diffusion on the actin occurs; clearly seen in Supplementary Movie 2c) and then bound to a forward site on the actin filament, completing one step. Thus, the hand-over-hand movement[12,13] including the intermediate process was directly visualised in high-resolution movies. Other behaviours of M5-HMM predicted by the 'inchworm'[20] and 'biased diffusion'[21] models were not observed at least within the time resolution used. The captured images clearly revealed that the forward movement is driven not by bending but by rotation of the L-head. The rotation appears to occur spontaneously after T-head detachment, suggesting that intramolecular tension driving the L-head swing exists in the two-head bound molecules.

Unfolding of coiled-coil tail

In a saturating amount of ADP, both heads were bound to a single actin filament and the L-head always appears nearly straight (curved slightly outward) (Fig. 2a, Supplementary Movie 3, and Supplementary Fig. 3b) as observed for M5-HMM moving in 0.1 μM and 1 μM ATP. In this nearly straight conformation, the neck domain appears to emerge from the rear of the motor domain[17]. During imaging of the two-head bound M5-HMM, we sometimes encountered unwinding of the short coiled-coil tail. After unwinding, the monomerised L-head immediately rotated toward the ARH orientation (Fig. 2b, Supplementary Movie 4). This head separation was rarely reversed

(Supplementary Movies 4c, d). This unwinding is unlikely to be caused by the tip-sample interaction because monomeric heads were detected in the earliest frames in the successive movies at new scan areas (see the latter half of Supplementary Movie 4b), and because a previous study showed the presence of a single-head fragment with an intact coiled-coil region in an expressed M5-HMM sample, although it was interpreted to be due to partial proteolysis[22]. Rather, this finding directly demonstrates that intramolecular tension exists in the two-head bound M5-HMM, and that the tension release caused by the unwinding results in the L-head rotation, similar to the L-head behaviour in the hand-over-hand movement. These observations provide the following important insights into the motor mechanism: (1) the neck-motor domain junction of L-head-ADP is sufficiently flexible to allow the head to strongly bind to actin in the R-ARH orientation, even without transitioning through a weak-binding ADP-Pi-bound state, (2) this strong binding forces the L-head into a strained 'pre-stroke' state, and (3) the L-head rotation is likely to occur spontaneously when the constraint holding the L-head in the strained state is removed by T-head detachment, suggesting that the lever swing by L-head is not accompanied by chemical transitions at the L-head.

Foot stomp in ATP

In general, during the acto-myosin ATPase cycle, the strained pre-stroke state is always formed after Pi is released from an ADP-Pi-bound head weakly interacting with actin[23]. Then, it may be considered that the strained pre-stroke state, which is formed directly by the binding of L-head-ADP to actin, does not participate in the forward step. We observed molecular behaviour in ATP that indicates that it does. In two-head bound M5-HMM, either of the motor domains frequently exhibited brief dissociation and reassociation on the same actin filament (or a brief translocation by ± ~5 nm along the actin filament), whereas M5-HMM remained at approximately the same position on the filament (as shown in Fig. 1 and Supplementary Fig. 3a; see Supplementary Movies 1, 2 and Methods). We have termed this behaviour 'foot stomp'. Note that when the T-head dissociates, it rarely rebinds to actin without stepping forward; thus, the T-head foot stomp is mostly observed as a brief translocation along the actin filament. The foot stomp was more frequently observed at the L-head than at the T-head (by a ratio of approximately 3:1, Fig. 3a). The briefly detached L-head does not carry bound Pi because Pi is rapidly released from an ADP-Pi-bound head when it attaches to actin[24]. Nevertheless, the detached L-head with only ADP bound rebinds to actin, still in the R-ARH orientation, and then swings forward following T-head detachment.

At each step, the L-head foot stomp occurred about twice in 0.1 μM ATP and 0.4

times in 1 μM ATP on average. These high frequencies of occurrence clearly indicate that a foot stomp at the L-head occurs while it is bound to ADP, not while it is bound to ADP-Pi. If Pi release, whose rate is independent of [ATP], was significantly delayed by the interaction of M5-HMM with the substrate surface containing 5% DPTAP, M5-HMM in high [ATP] would walk much more slowly than observed. Moreover, the foot stomp also occurs even when DPTAP is absent in the substrate. A foot-stomp-like behaviour was previously suggested in a fluorescence microscopy observation of walking M5 molecules[25]. Thus, the foot stomp is an inherent behaviour of M5. As will be described later, the foot stomp also occurs in ADP and under the nucleotide-free (NF) condition.

Conformational transition in L-head

Even under the NF condition, M5-HMM was bound to actin through the two heads (Fig. 2c, Supplementary Movie 5, and Supplementary Fig. 3c). However, unlike in the presence of nucleotides, the leading neck frequently exhibited a sharp bend conformation and alternated back and forth between the two conformations (Fig. 2c and Supplementary Fig. 3c), indicating that the two conformations are in equilibrium. The sharp bend conformation at the L-head was also observed recently by negative stain electron microscopy of acto-M5-HMM, although the chemical state was unspecified[17]. In the sharp bend conformation, both heads take the ARH orientation around the motor domain; thus both necks appear to emerge from the front of the respective motor domains. As will be clarified later, this sharp bending has no relevance to powerstroke generation but provides a useful indicator of whether or not the L-head contains ADP.

The proportions of the straight L-head detected (r) were 0.98 in 1 mM ADP and 0.36 under the NF condition (Fig. 3b). This finding is consistent with the ARH orientation distributions of single-headed M5 in the NF and ADP-bound conditions (Supplementary Fig. 4). In the NF condition, the orientation angle relative to the long axis of the actin filament was 34 ± 10° (mean ± s.d.) (although double-Gaussian distribution is somewhat significant: 33 ± 9° and 51 ± 7°; F-test, $p < 0.05$). In ADP, however, the angle was distributed more widely (29 ± 11° and 51± 15°; F-test, $p < 10^{-6}$), which may be relevant to two different ADP bound states in equilibrium[23]. Therefore, the hinge around the neck-motor domain junction of the ADP-bound head is more flexible than that of the NF head. Because of the relatively rigid hinge of the NF head, the leading neck in the R-ARH orientation tends to be sharply bent to release the large strain accumulated in the neck. This rigid hinge is also indicated by an observation that both heads are rarely bound to adjacent actin subunits predominantly in the NF condition

(Fig. 2d).

ADP release from L-head

In 1 μM ATP and even in 0.1 μM ATP, the leading neck was mostly straight (r ~ 0.98) (Fig. 3b), which suggests that the L-head retains ADP until the T-head binds to ATP and detaches from actin, consistent with previous reports[14,26-30]. From the proportion (Fig. 3b) and lifetime (Fig. 3c; see Supplementary Movie 6) of the straight L-head as a function of [ADP], we estimated the kinetic parameters for ADP binding/dissociation on the L-head: ADP dissociation constant $K_d\,(=k_-/k_+)$ = 0.075 ± 0.013 μM, ADP dissociation rate constant k_- = 0.100 ± 0.004 s^{-1}, and second-order ADP binding rate constant k_+ = 1.3 ± 0.3 $\mu M^{-1}s^{-1}$. The value of k_- is ~70 times smaller than the corresponding rate for the T-head (k_2 = 7.2 ± 1.5 s^{-1}) estimated above. This degree of asymmetry between the two heads is similar to that previously reported[26]. The value of k_+ is ~10 times smaller than the corresponding value of 12.6 $\mu M^{-1}s^{-1}$ previously measured in a solution study on single-headed M5[24]. The ADP dissociation rate constant of 0.100 s^{-1} means that, on average, one ADP is released from the L-head every 10 s. However, M5-HMM walks many steps during 10 s. Thus, we confirmed the consensus view that the sequential events of ADP release, the subsequent ATP binding, and the resulting head dissociation take place solely at the T-head, which is the basis for the processivity and hand-over-hand stroke generation[14,26-30]. Accordingly, the sharp bending observed at the NF L-head has no relevance to powerstroke generation.

Foot stomp in ADP and NF conditions

The foot stomp observed in ATP also occurred under all the nucleotide conditions examined here with higher frequencies at the L-head (Fig. 3a, Supplementary Fig. 5, and Supplementary Movies 3, 5). Note that in ADP and under the NF condition, complete detachment of the T-head was only sometimes observed. This detachment was followed by a forward step. This event was also counted as a foot stomp. The foot stomp at the T-head mostly occurred as brief translocation along actin. The frequency difference between the two heads became smaller when the L-head assumed a sharp bend conformation (~3:2 for L-head *vs* T-head). Thus, the frequency of foot stomping strongly correlates with the orientation of the bound head. Both heads would by nature preferentially take the ARH orientation. However, the nucleotide-bound L-head is forced to bind to actin in the R-ARH orientation and hence tends to detach from actin, leading to a more frequent foot stomping. This implies that the L-head would be less

susceptible to catalytic activation by actin, possibly contributing to some extent to the asymmetry in the kinetic constants between the two heads.

Discussion

In general, the conformational change in myosin upon the hydrolysis of bound ATP to ADP-Pi is a recovery stroke (*i.e.*, post-stroke to pre-stroke state transition), and the actin-activated Pi release from ADP-Pi reverses the head conformation to produce a forward force[23]. However, a forward force (or the strained pre-stroke state) can also be produced by the direct binding of the ADP-bound L-head to actin. In ATP, the force that is produced in this way after a foot stomp at the L-head drives lever-arm swing. The number of foot stomp events at the L-head per a step is around 1 only in low [ATP]. However, this type of force generation is likely to take place also in high [ATP] under a loaded condition. Moreover, this force generation mechanism suggests that the ADP-bound head has the potential to repeatedly produce a force when an appropriate backward force is applied. This potential was recently indicated by an optical-trap-based experiment on a single M5 head interacting with actin under a certain backward load[31]. The powerstroke is reversed and actin-bound pre- and post stroke conformations are repeated before completing one ATPase cycle. In Supplementary Figure 6, we propose a model for the chemomechanical cycle of M5 based on previous studies and the new findings obtained here.

As demonstrated here, previously known and unknown behaviours of M5-HMM clearly appear in the molecular movies. Unlike previous methods, high-resolution AFM imaging unselectively provides the comprehensive information on the structure and dynamics of a functioning molecule. Thus, the HS-AFM imaging of functioning biomolecules has the potential to transform the fields of structural biology and single-molecule biology.

Methods Summary

M5-HMM was prepared from chick brain, and partially biotinylated actin filaments were prepared and then stabilised with phalloidin[11]. Biotin-containing lipid bilayers were formed on a mica surface[8]. The biotinylated actin filaments were immobilised on the bilayer surface and then a solution of M5-HMM was deposited on the surface. All imaging experiments were performed in the tapping mode using a laboratory-built HS-AFM apparatus[2,3].

Full Methods and any associated references are available in the online version of the paper at www.nature.com/nature.

References

1. Joo, C. *et al*. Advances in single-molecule fluorescence methods for molecular biology. *Annu. Rev. Biochem*. **77**, 51-76 (2008).
2. Ando, T., Uchihashi, T. & Fukuma, T. High-speed atomic force microscopy for nano-visualization of dynamic biomolecular processes. *Prog. Surf. Sci*. **83**, 337–437 (2008).
3. Ando, T. *et al*. A high-speed atomic force microscope for studying biological macromolecules. *Proc. Natl. Acad. Sci. USA* **98**, 12468–12472 (2001).
4. Hansma, P. K., Schitter, G., Fantner, G. E. & Prater, C. High-speed atomic force microscopy. *Science* **314**, 601–602 (2006).
5. Viani, M. B. *et al*. Probing protein-protein interactions in real time. *Nat. Struct. Biol*. **7**, 644–647 (2000).
6. Shibata, M. *et al*. High-speed atomic force microscopy shows dynamic molecular processes in photo-activated bacteriorhodopsin. *Nat. Nanotech*. **5**, 208–212 (2010).
7. Yamashita, H. *et al*. Dynamics of bacteriorhodopsin 2D crystal observed by high-speed atomic force microscopy. *J. Struct. Biol*. **167**, 153–158 (2009).
8. Yamamoto, D., Uchihashi, T., Kodera, N. & Ando, T. Anisotropic diffusion of point defects in two-dimensional crystal of streptavidin observed by high-speed atomic force microscopy. *Nanotechnology* **19**, 384009 (9 pp) (2008).
9. Sellers, J. R. & Weisman, L. S. in *Myosins: A Superfamily of Molecular Motors, Proteins and Cell Regulation* (ed. Coluccio, L.) 289–324 (Springer, 2008).
10. Metha, D. *et al*. Myosin-V is a processive actin-based motor. *Nature* **400**, 590–593 (1999).
11. Sakamoto, T., Amitani, I., Yokota, E. & Ando, T. Direct observation of processive movement by individual myosin V molecules. *Biochem. Biophys. Res. Commun*. **272**, 586–590 (2000).
12. Yildiz, A. *et al*. Myosin V walks hand-over-hand: single fluorophore imaging with 1.5 nm localization. *Science* **300**, 2061–2065 (2003).
13. Forkey, J. N. *et al*. Three-dimensional structural dynamics of myosin V by single-molecule fluorescence polarization. *Nature* **422**, 399–404 (2003).
14. Sakamoto, T. *et al*. Direct observation of the mechanochemical coupling in myosin Va during processive movement. *Nature* **455**, 128–132 (2008).

15. Walker, M. L. *et al*. Two-headed binding of a processive myosin to F-actin. *Nature* **405**, 804–807 (2000).
16. Burgess, S. *et al*., The prepower stroke conformation of myosin V. *J. Cell Biol.* **159**, 983–991 (2002).
17. Oke, O. A. *et al*., Influence of lever structure on myosin 5a walking. *Proc. Natl. Acad. Sci. USA* **107**, 2509–2514 (2010).
18. Baker, J. E. *et al*. Myosin V processivity: multiple kinetic pathways for head-to-head coordination. *Proc. Natl. Acad. Sci. USA* **101**, 5542–5546 (2004).
19. Huxley, H. E. The mechanism of muscular contraction. *Science* **164**, 1356–1365 (1969).
20. Hua, W., Chung, J. & Gelles, J. Distinguishing inchworm and hand-over-hand processive kinesin movement by neck rotation measurements. *Science* **295**, 844–848 (2002).
21. Okada, T. *et al*. The diffusive search mechanism of processive myosin class-V motor involves directional steps along actin subunits. *Biochem. Biophys. Res. Commun*. **354**, 379–384 (2007).
22. Wang, F. *et al*. Effect of ADP and ionic strength on the kinetic and motile properties of recombinant mouse myosin V. *J. Biol. Chem*. **275**, 4329−4335 (2000).
23. Geeves, M. A. & Holmes, K. C. Structural mechanism of muscle contraction. *Annu. Rev. Biochem*. **68**, 687–728 (1999).
24. De La Cruz, E. M. *et al*. The kinetic mechanism of myosin V. *Proc. Natl. Acad. Sci. USA* **96**, 13726–13731 (1999).
25. Syed, S. *et al*. Adaptability of myosin V studied by simultaneous detection of position and orientation. *EMBO. J*. **25**, 1795–1803 (2006).
26. Rosenfeld, S. S. & Sweeney, H. L. A model of myosin V processivity. *J. Biol. Chem*. **279**, 40100–40111 (2004).
27. Veigel, C., Schmitz, S., Wang, F. & Sellers, J. R. Load-dependent kinetics of myosin-V can explain its high processivity. *Nat. Cell Biol*. **7**, 861–869 (2005).
28. Oguchi, Y. *et al*. Load-dependent ADP binding to myosins V and VI: implications for subunit coordination and function. *Proc. Natl. Acad. Sci. USA* **105**, 7714–7719 (2008).
29. Purcell, T. J., Sweeney, H. L. & Spudich, J. A. A force-dependent state controls the coordination of processive myosin V. *Proc. Natl. Acad. Sci. USA* **102**, 13873–13878 (2005).
30. Forgacs, E. *et al*. Kinetics of ADP dissociation from the trail and lead heads of actomyosin V following the power stroke. *J. Biol. Chem.* **283**, 766–773 (2008).

31. Sellers, J. R. & Veigel, C. Direct observation of the myosin-Va power stroke and its reversal. *Nat. Struct. Mol. Biol.* **17,** 590–595 (2010).

End Notes

Supplementary Information is linked to the online version of the paper at www.nature.com/nature.

Acknowledgements We thank T. Uchihashi and H. Yamashita for technical assistance and discussion, and J. Sellers for critical reading of the draft and for valuable comments. This work was supported by CREST/JST, Special Coordination Funds for Promoting Science and Technology (Effective Promotion of Joint Research with Industry, Academia, and Government) from JST, a Grant-in-Aid for Basic Research (S) from JSPS, and Knowledge Cluster/MEXT.

Author Contributions N.K. performed the high-speed AFM experiments and data analysis and wrote the first draft of the manuscript. D.Y. and N.K. developed the lipid bilayer-based assay system. R.I. participated in the sample preparations in the early stage of this study. T.A. and N.K. developed the instrument. T.A. concepted the experiment and prepared the final manuscript.

Author information Reprints and permissions information is available at www.nature.com/reprints. The authors declare no competing financial interests. Correspondence and requests for materials should be addressed to T.A. (tando@kenroku.kanazawa-u.ac.jp).

Figure Legends

Figure 1 | Directly visualised walking M5-HMM. (a) Successive AFM images showing processive movement of M5-HMM in 1 μM ATP (Supplementary Movie 1). Arrowhead, a streptavidin molecule; arrows, the coiled-coil tail of M5-HMM tilted toward the minus end of actin. Scan area, 130 × 65 nm^2; scale bar, 30 nm. (b) Schematic for two-head bound M5-HMM. (c) Schematic explaining the images in (d) and (e). (d), (e) Successive AFM images showing hand-over-hand movement (Supplementary Movie 2). The swinging lever is highlighted with thin lines. (d) In 1 μM ATP. Scan area, 150 × 75 nm^2; scale bar, 50 nm. (e) In 2 μM ATP. Scan area, 130 × 65 nm^2; scale bar, 30 nm. Vertical dashed lines (in a, d, e), the centres of mass of the motor domains. All images

were taken at 146.7 ms frame^{-1}.

Figure 2 | AFM images of M5-HMM in ADP and under NF condition. (a) Successive AFM images taken in 50 μM ADP (Supplementary Movie 3). (b) Successive AFM images showing unwinding of short coiled-coil tail of two-head bound M5-HMM observed in 50 μM ADP (Supplementary Movie 4). (c) Successive AFM images taken under the NF condition (see Supplementary Movie 5). (d) AFM image and illustration of NF M5-HMM with heads bound to adjacent actin subunits (top). All images (a-d) were taken at 333.2 ms frame^{-1} with a scan size of 90 × 90 nm^2. The plus ends of the actin filaments are indicated by '+' and the scale bars are 30 nm (a-d).

Figure 3 | Foot stomp and L-head conformations in different nucleotide conditions. (a), (b) Proportion of foot stomp frequencies observed at L- and T-heads (a) and of detected straight and sharp bend conformations of L-head (b). The numbers in {steps}, <events>, [molecules], and (frames) represent the respective numbers examined using images within which both heads were fully located. 'Long run' represents data obtained using wide imaging areas. (c) Average lifetimes of L-head with straight conformation in various [ADP]. The numbers in brackets represent the total numbers of straight-to-bend transition events observed with ~50 different molecules under the respective [ADP]. The inset shows the reaction scheme (ST, NF straight L-head; ST_{ADP}, ADP-bound straight L-head; BN, sharply bent NF L-head). Error bars, ± s.e.m; $k_{S\text{-}B}$ = 0.32 ± 0.02 s^{-1} (best-fit value ± s.d.).

Methods

Protein purification and reagents. M5-HMM was prepared from chick brain[32]. Partially biotinylated (20%) actin filaments were prepared and then stabilized with phalloidin[11]. Streptavidin, synthetic lipids, apyrase, and hexokinase were purchased from Wako Pure Chemical (Osaka, Japan), Avanti Polar Lipids (Alabama, USA), Sigma-Aldrich (Missouri, USA), and Roche Diagnostics (Basel, Switzerland), respectively.

Preparation of samples for AFM observation. Biotin-containing lipid bilayers were formed on a mica surface[8,33]. A typical lipid composition was 1,2-dipalmitoyl-*sn*-glycero-3-phosphocholine (DPPC), 1,2-dipalmitoyl-3-trimethylammonium-propane (DPTAP), and 1,2-dipalmitoyl-*sn*-glycero-3-phosphoethanolamine-N-(cap biotinyl) (biotin-cap-DPPE)

with a weight ratio of 0.85:0.05:0.1. In some cases, the content of the positively charged lipid DPTAP was reduced. After rinsing the lipid bilayer substrate with buffer A (20 mM imidazole-HCl, pH 7.6, 25 mM KCl, 2 mM $MgCl_2$, 1 mM EGTA, 5 mM DTT), a drop (2 μl) of streptavidin in buffer A (10 nM) was deposited on the substrate for 3 min. In some experiments, additional streptavidin molecules (2 μl of 40 nM) were deposited on the surface for 2 min. After rinsing with buffer A, a drop (2 μl) of partially biotinylated actin filaments (1 μM) in buffer A was deposited on the lipid bilayers for 10 min. After rinsing with a solution containing either 0.1 μM – 1 mM ATP, 0.1 μM – 1 mM ADP (1 U ml^{-1} hexokinase and 10 mM glucose were added in the case of 1 mM ADP to remove contaminating ATP) or 1 U ml^{-1} apyrase (to ensure the NF condition) in buffer A, a drop (2 μl) of the same solution plus M5-HMM (0.1 – 1 nM) was deposited on the lipid bilayers for 3 min. Finally, the sample was attached to the scanning stage of a HS-AFM apparatus and immersed in the same solution (~60 μl) without M5-HMM. When the lipid bilayers did not contain the positively charged lipid DPTAP, we further added M5-HMM to the observation solution.

HS-AFM apparatus and cantilevers. We used a laboratory-built tapping-mode HS-AFM apparatus[2,3] together with small cantilevers designed for HS-AFM (spring constant, 0.1 – 0.2 N m^{-1}; resonant frequency, 0.8 – 1.2 MHz; quality factor, ~ 2 in water)[34]. The probe tip was grown on the tip of a cantilever by electron beam deposition and was further sharpened by argon plasma etching[2]. In the best case, a tip apex radius of ~4 nm was achieved. To achieve a small tip-sample loading force, the free oscillation peak-to-peak amplitude of the cantilever (A_0) was set to 1.5 – 2.5 nm and the amplitude set-point was set at larger than 0.9 × A_0. Note that the mechanical quantity that affects the sample is not the force itself but the force impulse, *i.e.*, the product of force and the time over which the force acts. In tapping-mode HS-AFM, the time of force action is short (~100 ns), and therefore, a relatively large peak force (~20 pN) would not affect the sample significantly. The all imaging experiments could be routinely conducted without difficulty except for the occasional deterioration of image quality owing to tip smear or cracking which was difficult to control. The tip smearing was caused by the attachment of molecules contained in the sample but the molecules were sometimes removed during imaging. The cracking of the sharp tip yields a double image of every object, as shown in Supplementary Movie 6.

HS-AFM imaging and processive run. All observations were performed at room temperature (24 – 26 °C). To facilitate rapid imaging of moving M5-HMM molecules on actin, sample areas in which actin filaments were aligned approximately parallel to the x-direction were chosen. M5 walks approximately straight along actin filaments as

the two heads span the actin filament helical pseudorepeat of ~36 nm[10,12-15]. This property and the high-precision feedback system of the instrument[2,35] facilitate the continuous imaging of walking M5-HMM molecules weakly adsorbed sideways onto the DPTAP-containing substrate surface. In the absence of DPTAP in the substrate, M5-HMM molecules often walked on the top surface of actin filaments. In this case, it was difficult to acquire high-resolution images since AFM is inefficient for visualising molecules not supported on a surface.

High-resolution imaging of moving M5-HMM: To obtain high-resolution images of M5-HMM molecules translocating along actin in 0.1 – 2 μM ATP, the scan area was narrowed (to typically about 130 × 65 nm^2) and the number of pixels was optimized (80 × 40 or 80 × 50) such that the phase delay in tracing the sample surface was minimised and the imaging rate (146.7 ms/frame) was sufficiently high to capture the moving molecules. When long processive runs (~15 steps) in 0.1 – 2 μM ATP were observed, the molecules were tracked by shifting the narrow scan area manually (mainly in the x-direction). The tracking could not sometimes be continued when the target molecule collides with a molecule walking ahead, a portion of discontinuous substrate surface was encountered, or the manual tracking by an operator was not appropriately made. It is not owing to the tip-sample interaction.

Velocity measurements: In the experiment to determine the translocation velocity of M5-HMM in various [ATP], the scan areas (400 × 125 nm^2) were fixed and images were captured at 146.3 ms $frame^{-1}$. To facilitate rapid imaging for this relatively wide scan area, the number of pixels was reduced to 80 × 25 (thus, the scan velocity in the x-direction is only slightly higher than that in high-resolution imaging mentioned above). The image quality was generally lowered but was sufficiently high to identify M5-HMM molecules on actin. When translocation velocity was too high to capture every dwelled molecule, its translocation velocity was determined using at least four different dwell positions where the molecules were captured on video.

Imaging for detecting foot stomp and L-head conformations: In the experiment to analyse foot stomping and L-head conformations in ADP and under the NF conditions, the imaging was carried out at a rate of 333.2 ms $frame^{-1}$ using fixed imaging areas (typically 90 × 90 nm^2 with 80 × 80 pixels). In the experiment to analyse foot stomping and L-head conformations in ATP, the imaging was carried out at a rate of 146.7 ms $frame^{-1}$ using two scan modes. In one mode, the imaging areas were fixed (typically at 130 × 65 nm^2 with 80 × 40 pixels). M5-HMM molecules that entered the imaging areas were captured on video. In the other mode, a translocating M5-HMM molecule was tracked by shifting the scan area (typically 130 × 65 nm^2 with 80 × 40 pixels).

Image analysis. A Gaussian filter for removing spike noises and a flattening filter for removing the substrate-tilt effect were applied to each AFM image. Each position of the motor domain of M5-HMM was determined by calculating the centre of mass to measure its displacement. The following events were considered as a foot stomp: (1) an entire head disappears and then reappears at approximately the same position, (2) either motor domain of a two-head bound M5-HMM molecule is translocated by ± ~5 nm along the actin filament, and (3) a motor domain disappears while its neck domain is visible (*i.e.*, the head detaches while scanning the region where the motor domain was attached in the previous frame scan and then rebinds to actin). Moreover, when an entire T-head disappeared in ADP and under the NF conditions, the molecule sometimes stepped forward. This event was also counted as a foot stomp. Note that a foot stomp was also observed even when the substrate surface did not contain DPTAP, although we did not systematically analyse it. When the L-head is sharply bent, the neck-neck junction becomes closer to the bound actin filament (and hence, the space surrounded by the two heads and actin becomes narrower). We identified the sharp bend conformation by visual observation of these features. For the quantitative analysis of foot stomp events and L-head conformations in ATP, we analysed only images within which both heads were fully located before and after a step. Therefore, the steps that actually observed were more than those shown in Fig. 3a, b.

Kinetic analysis of conformational change at L-head. The proportion of the straight L-head conformation detected (r) as a function of [ADP] (Fig. 3b) was analysed to estimate the ADP dissociation constant for the L-head (K_d) using the relationship

$$r([ADP]) = \frac{r_D \cdot [ADP] + r_{NF} \cdot K_d}{[ADP] + K_d}, \quad \text{(eq. 1)}$$

where r_D = 0.98 and r_{NF} = 0.36 are the proportion of the straight L-head detected in a saturating amount of ADP and in the NF condition, respectively. Considering the reaction scheme (Fig. 3c, inset), the average lifetime of the straight L-head, $<\tau_{ST}>$, is approximately expressed as

$$< \tau_{ST} > = n_{NF} / \left(k_{S-B} + \frac{k_- k_+ [ADP]}{k_- + k_+ [ADP]} \right) + n_{ADP} / \left(k_- + \frac{k_- k_{S-B}}{k_- + k_{S-B}} \right), \quad \text{(eq. 2)}$$

where k_{S-B} represents the spontaneous straight-to-sharp bend transition rate for the NF L-head, n_{NF} and n_{ADP} are the fractions of NF L-head and ADP-bound L-head at a given [ADP], respectively, which are calculated using K_d = 0.075 μM, and k_- and k_+ are the ADP dissociation rate constant and ADP association rate constant at the L-head,

respectively. Using eq. 2, the observed $<\tau_{ST}>$ as a function of [ADP] (Fig. 3c) was analysed to estimate k_{S-B}, k_{-}, and k_{+}.

32. Koide, H. *et al*. Identification of the single specific IQ motif of myosin V from which calmodulin dissociates in the presence of Ca^{2+}. *Biochemistry* **45**, 11598–11604 (2006).
33. Yamamoto, D. *et al*. High-speed atomic force microscopy techniques for observing dynamic biomolecular processes. *Methods Enzymol*. **475**(B), 541–564 (2010).
34. Kitazawa, M., Shiotani, K. & Toda, A. Batch fabrication of sharpened silicon nitride tips. *Jpn. J. Appl. Phys.* **42**, 4844–4847 (2003).
35. Kodera, N., Sakashita, M. & Ando, T. Dynamic proportional-integral-differential controller for high-speed atomic force microscopy. *Rev. Sci. Instrum.* **77,** 083704 (7 pp) (2006).

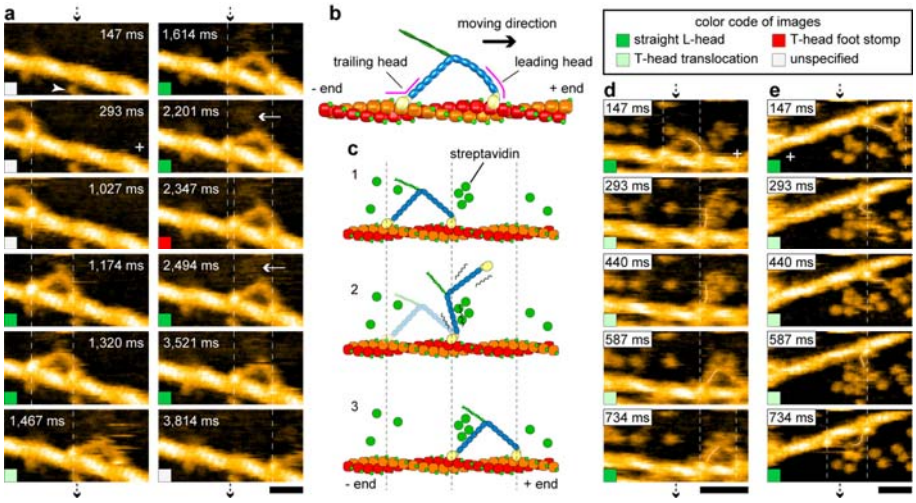

Figure 1

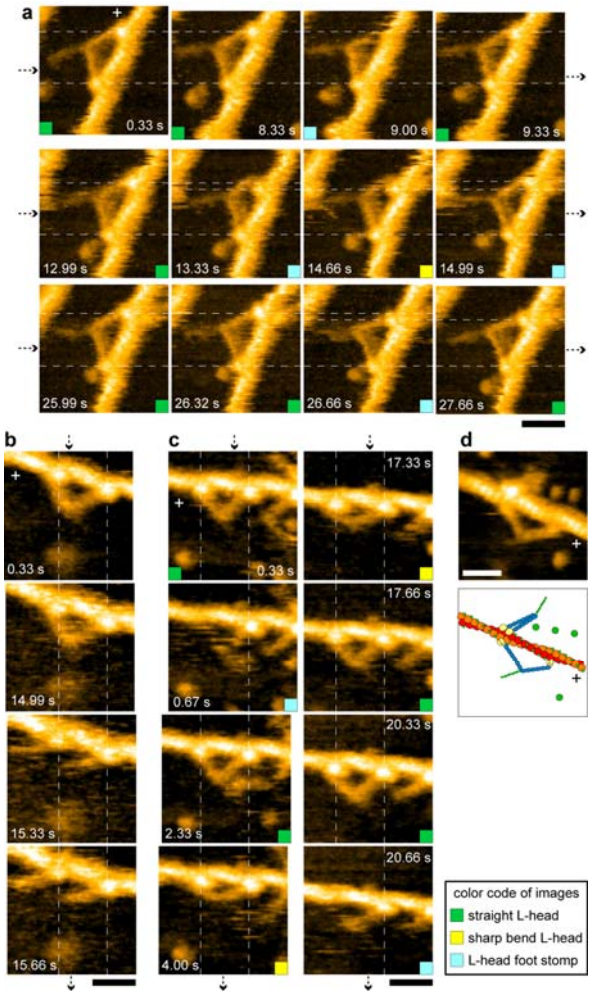

Figure 2

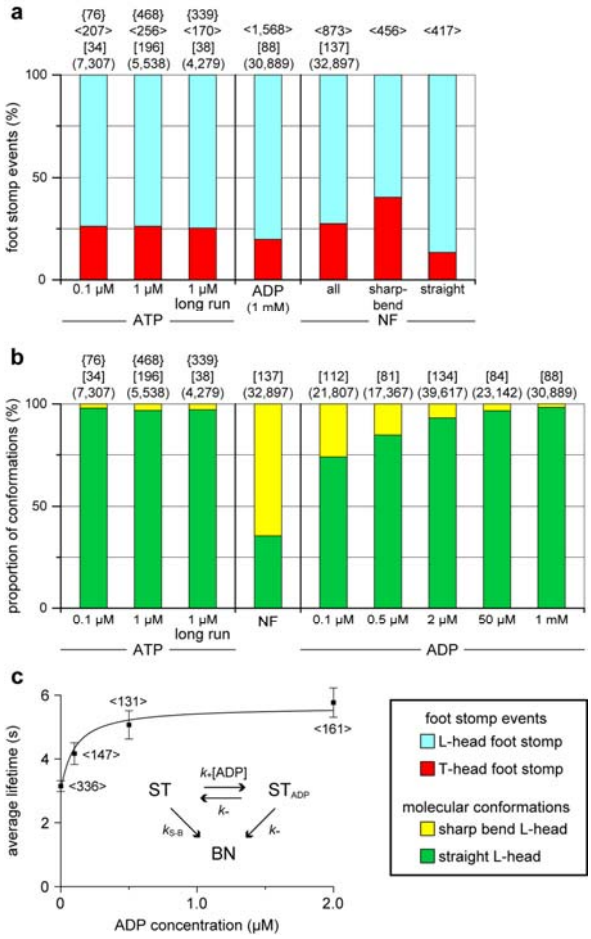
a
{76} <207> [34] (7,307)
{468} <256> [196] (5,538)
{339} <170> [38] (4,279)
<1,568> [88] (30,889)
<873> [137] (32,897)
<456>
<417>
foot stomp events (%)
100
50
0
0.1 μM
1 μM
1 μM long run
ADP (1 mM)
all
sharp-bend
straight
ATP
NF
b
{76} [34] (7,307)
{468} [196] (5,538)
{339} [38] (4,279)
[137] (32,897)
[112] (21,807)
[81] (17,367)
[134] (39,617)
[84] (23,142)
[88] (30,889)
proportion of conformations (%)
0.1 μM
1 μM
1 μM long run
NF
0.1 μM
0.5 μM
2 μM
50 μM
1 mM
ATP
ADP
c
average lifetime (s)
6
4
2
0
<131>
<161>
<147>
<336>
ST
k_+[ADP]
k_-
ST_{ADP}
k_{S-B}
k_-
BN
0
1.0
2.0
ADP concentration (μM)
foot stomp events
L-head foot stomp
T-head foot stomp
molecular conformations
sharp bend L-head
straight L-head

Figure 3